ATR and Rad17 collaborate in modulating Rad9 localisation at sites of DNA damage

Annette L. Medhurst[1,*], Daniël O. Warmerdam[2,*], Ildem Akerman[1], Edward H. Verwayen[2], Roland Kanaar[2,3], Veronique A. J. Smits[2,‡,§] and Nicholas D. Lakin[1,§]

[1]Department of Biochemistry, University of Oxford, South Parks Road, Oxford, OX1 3QD, UK
[2]Department of Cell Biology and Genetics, Cancer Genome Center and [3]Department of Radiation Oncology, Erasmus MC, PO Box 2040, 3000 CA Rotterdam, The Netherlands

*These authors contributed equally to this work
‡Present address: Unidad de Investigación, Hospital Universitario de Canarias, Ofra s/n, La Cuesta, 38320, Tenerife, Spain
§Authors for correspondence (e-mails: vsmits@ull.es; nicholas.lakin@bioch.ox.ac.uk)

Accepted 2 September 2008
Journal of Cell Science 121, 3933-3940 Published by The Company of Biologists 2008
doi:10.1242/jcs.033688

Summary

The cell cycle checkpoint kinase Chk1 is phosphorylated and activated by ATR in response to DNA damage and is crucial for initiating the DNA damage response. A number of factors act in concert with ATR to facilitate Chk1 phosphorylation, including Rad17-RFC, the Rad9-Rad1-Hus1 complex, TopBP1 and Claspin. Rad17 is required for loading of Rad9-Rad1-Hus1 (9-1-1) onto sites of DNA damage. Although phosphorylation of Rad17 by ATR is required for checkpoint function, how this affects 9-1-1 regulation remains unclear. We report that exposure of cells to DNA damage or replication stress results in Rad17-dependent immobilisation of Rad9 into nuclear foci. Furthermore, expression of mutant Rad17 that cannot be phosphorylated by ATR (Rad17^{AA}), or downregulation of ATR, results in a decreased number of cells that display Rad9 foci. Photobleaching experiments reveal an increase in the dynamic behaviour of Rad9 within remaining foci in the absence of ATR or following expression of Rad17^{AA}. Together, these data suggest a model in which Rad17 and ATR collaborate in regulating Rad9 localisation and association at sites of DNA damage.

Supplementary material available online at
http://jcs.biologists.org/cgi/content/full/121/23/3933/DC1

Key words: ATR, DNA-damage signalling, Cell cycle checkpoints, Genome stability, Rad9

Introduction

Proteins involved in signalling DNA damage are critical for maintaining genome stability and guard against a variety of disease states including a predisposition to malignancy (Kastan and Bartek, 2004). Consequently, the cell has evolved a comprehensive and intricate network of pathways that act in concert to detect and signal DNA damage for subsequent processing and repair. The phosphatidylinosotol (PI)-3 kinase-related kinases (PIKKs) ATM (ataxia telangiectasia mutated) and ATR (ATM- and Rad3-related) function in distinct but partially overlapping pathways activated in response to genotoxic stress. ATM and ATR are recruited to sites of DNA damage, become activated, and subsequently phosphorylate a number of proteins that regulate various aspects of the DNA damage response (DDR). Although ATM is the principal kinase responsible for detecting and signalling DNA double-strand breaks (DSBs), ATR responds to a wider variety of DNA damage architectures including UV-induced base damage, replication stress and DNA DSBs (Abraham, 2001; Adams et al., 2006; Jazayeri et al., 2006). ATR phosphorylates and activates the Chk1 kinase in response to genotoxic stress. Chk1 then proceeds to phosphorylate a variety of proteins that regulate aspects of the DDR, including cell cycle arrest, stabilisation of stalled replication forks and DNA repair (Chen and Sanchez, 2004). As such, the ATR-Chk1 axis is central to the DDR and crucial for maintaining genome integrity. For example, hypomorphic mutations in the *ATR* gene result in Seckel syndrome, a rare disease characterised by developmental abnormalities and genome instability (O'Driscoll et al., 2003).

The principal DNA architecture recognised by ATR is single-stranded DNA (ssDNA) generated by either nucleases processing sites of DNA damage (Adams et al., 2006; Jazayeri et al., 2006; Zou and Elledge, 2003), or uncoupling of the replicative helicase from stalled replication forks (Byun et al., 2005). Regions of ssDNA are subsequently coated by the ssDNA protein binding complex RPA (replication protein A), which facilitates the recruitment of ATR to sites of DNA damage through an interaction with the ATR-associated protein ATRIP (Ball et al., 2005; Zou and Elledge, 2003). Although recognition of ssDNA by ATR is crucial in allowing this kinase to phosphorylate and activate Chk1, a number of other factors are required for this event. For example, disruption of either Rad17 or components of the Rad9-Rad1-Hus1 (9-1-1) complex results in defective phosphorylation of Chk1 in response to DNA damage (Melo and Toczyski, 2002). Rad17 along with the four small subunits of replication factor C (RFC2-5) acts as a clamp loader of 9-1-1 at or near sites of DNA damage (Bermudez et al., 2003; Ellison and Stillman, 2003; Zou et al., 2002). Similarly to ATR, Rad17/9-1-1 is also recruited to ssDNA coated with RPA (Zou et al., 2003). However, Rad17/9-1-1 and ATR are recruited to DNA damage independently, arguing against these two DNA damage sensors acting in a linear pathway with regard to activation of Chk1 (Kondo et al., 2001; Melo et al., 2001; Zou et al., 2002). Instead, 9-1-1 activates ATR by recruiting the ATR-activating protein TopBP1 to DNA damage (Delacroix et al., 2007; Kumagai et al., 2006; Lee et al., 2007). The final step in Chk1 activation is phosphorylation of Claspin by ATR, which provides docking sites for Chk1 recruitment

and subsequent phosphorylation by ATR (Kumagai and Dunphy, 2003).

Although a unified view of how Rad17, 9-1-1 and ATR access sites of DNA damage and facilitate Chk1 activation is beginning to emerge, how these proteins act in concert to propagate and maintain the checkpoint response remains unclear. Phosphorylation of Rad17 by ATR on Ser635 and Ser645 is required for cells to initiate cell cycle arrest following DNA damage (Bao et al., 2001). However, the molecular basis of how ATR-mediated Rad17 phosphorylation influences the 9-1-1 complex once it has accessed sites of DNA damage remains largely unexplored. Here we assess the impact of ATR on 9-1-1 complex regulation once it has accumulated at sites of DNA damage, and provide data that support a role for ATR-mediated Rad17 phosphorylation in maintaining Rad9 at sites of genotoxic stress.

Results

A fraction of Rad9 is converted into an immobile pool within nuclei in response to DNA damage and replication stress

To gain a greater understanding of the events required for regulation of 9-1-1, we examined the enrichment of Rad9 in nuclear foci in response to DNA damage or replication stress. When examining endogenous Rad9 by immunofluorescence, we observed a diffuse nuclear distribution of this protein in untreated human and mouse cells that relocated to discrete nuclear retained foci in response to UV radiation and aphidicolin treatment (Fig. 1A). To assess formation of Rad9 foci in live cells, we generated a cell line that stably expressed Rad9 tagged with eGFP-HA (GFP-Rad9) (Fig. 1B). GFP-Rad9 runs as multiple bands on SDS-PAGE, as observed by others (Zou et al., 2002), which partially represents the phosphorylation status of the protein (data not shown). GFP-Rad9 co-immunoprecipitated with endogenous Hus1 and Rad1 (Fig. 1C). Furthermore, cells expressing GFP-Rad9 retained the ability to phosphorylate Chk1 in response to UV-induced DNA damage (Fig. 1D) and did not display an increased sensitivity to DNA-damaging agents (data not shown). Together, these data indicate that GFP-Rad9 interacts with its functionally important partners and does not interfere with the DDR. Similarly to endogenous Rad9, GFP-Rad9 was equally distributed throughout the nucleus in unperturbed cells and relocated into nuclear foci in response to UV or aphidicolin treatment. The majority of these foci appeared throughout the nucleus, but in a subset of the cells the foci were localised at the nuclear periphery (Fig. 1E). UV-induced GFP-Rad9 foci became apparent between 10 and 30 minutes following irradiation (data not shown) and colocalised with RPA (Fig. 1F), indicating that GFP-Rad9 is recruited to sites of ssDNA generated in response to DNA damage.

Rad17 phosphorylation is required for Rad9 to form foci in response to DNA damage and replication stress

Although ATR-mediated phosphorylation of Rad17 on Ser635 and Ser645 is required for checkpoint activation (Bao et al., 2001), how this affects the ability of the 9-1-1 complex to access and be retained at sites of DNA damage remains unclear. For example, loading of 9-1-1 onto sites of DNA damage occurs independently of ATR, arguing that ATR-mediated Rad17 phosphorylation is not required for 9-1-1 to access sites of DNA damage (Kondo et al., 2001; Lisby et al., 2004; Melo et al., 2001; You et al., 2002; Zou et al., 2002). Conversely, DNA damage-induced phosphorylation of Rad17 has been reported to promote the interaction of this protein with the 9-1-1 complex (Bao et al., 2001), suggesting that ATR affects the ability of 9-1-1 to interact with sites of DNA damage.

To assess how Rad17 contributes to the ability of 9-1-1 to interact with sites of DNA damage, we examined the requirement for ATR-

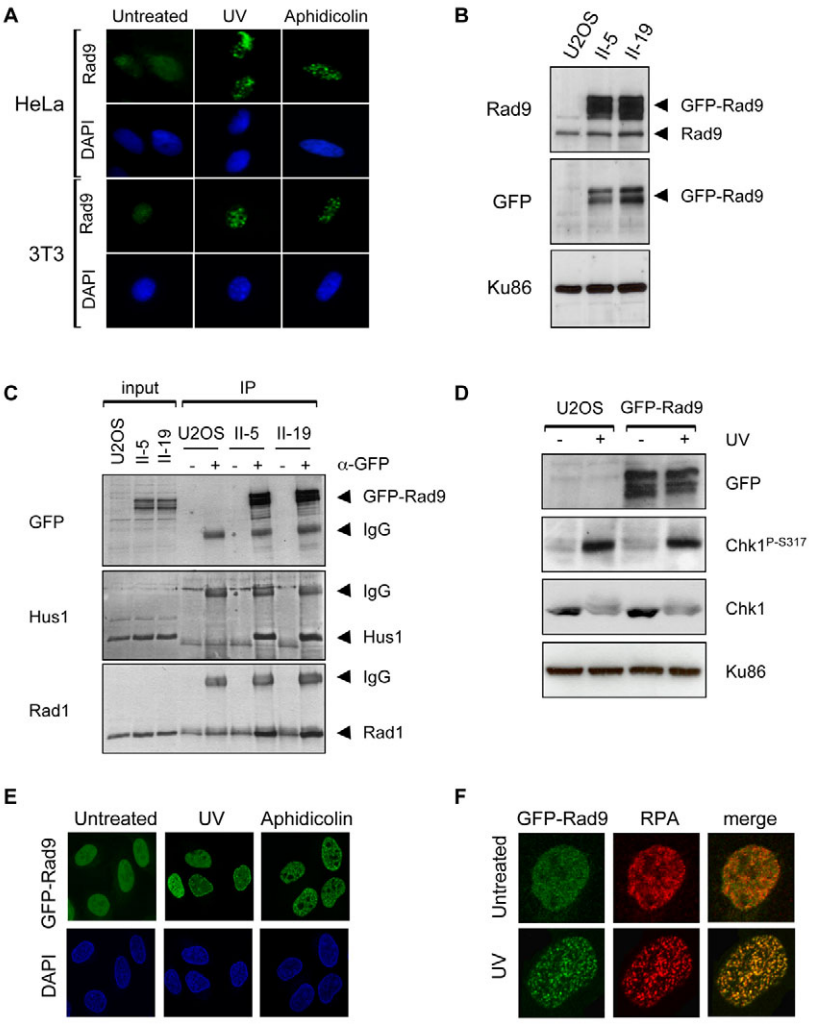

Fig. 1. Rad9 accumulates in nuclear foci in response to genotoxic stress. (A) HeLa and Swiss 3T3 cells were left untreated, exposed to UV, or treated with aphidicolin. Rad9 was visualised by immunofluorescence. (B) Western blot analysis of untransfected U2OS cells or different U2OS clones stably expressing GFP-Rad9 (II-5 and II-19), using the indicated antibodies. (C) U2OS cells or clones expressing GFP-Rad9 (II-5 and II-19) were lysed and GFP-Rad9 immunoprecipitated using anti-GFP antibodies. The presence of associated proteins was analysed by immunoblotting with the indicated antibodies. (D) U2OS cells or cells expressing GFP-Rad9 were either left untreated or exposed to UV. After 1 hour, cells were lysed, and western blot analysis was performed using the indicated antibodies. (E) U2OS cells expressing GFP-Rad9 were left untreated, exposed to UV, or treated with aphidicolin. GFP-Rad9 was visualised by direct fluorescence. (F) U2OS cells expressing GFP-Rad9 were left untreated or exposed to UV. GFP-Rad9 was detected by direct fluorescence and RPA (p34 subunit) by immunofluorescence.

mediated phosphorylation of Rad17 to allow Rad9 to accumulate in nuclear foci following genotoxic stress. Repression of Rad17 expression by siRNA resulted in a decrease from 35% to 10% of HeLa cells that displayed aphidicolin-induced Rad9 foci compared with cells transfected with a control oligonucleotide (Fig. 2A). A similar dependence on Rad17 was observed for UV- or aphidicolin-induced GFP-Rad9 foci formation (data not shown). To assess how phosphorylation of Rad17 by ATR affects Rad9 foci formation, we generated Flag-Rad17 and Flag-Rad17^{AA} (in which the Ser635 and Ser645 ATR phosphorylation sites were substituted with alanine). When introduced into U2OS cells expressing GFP-Rad9, Flag-Rad17 and Flag-Rad17^{AA} were present in chromatin-enriched cellular fractions independently of replication stress, confirming that the Flag-tag does not interfere with the DNA binding properties of these proteins (Fig. 2B). Neither siRNA-mediated knockdown of Rad17, nor overexpression of Flag-Rad17^{AA} dramatically affected cell cycle progression in U2OS cells (supplementary material Fig. S1). In cells transfected with empty expression vector, phosphorylation of endogenous Rad17 at Ser645 increased in response to aphidicolin (Fig. 2B). Although aphidicolin-induced phosphorylation of Rad17 at Ser645 remained apparent in cells expressing Flag-Rad17, this was reduced in cells transfected with Flag-Rad17^{AA} (Fig. 2B), confirming the dominant-negative nature of this mutant (Bao et al., 2001).

To assess Rad9 foci in cells that express Flag-Rad17 or Flag-Rad17^{AA}, we introduced these proteins into U2OS cells stably expressing GFP-Rad9 using a low efficiency transfection procedure. Scoring Flag-negative or Flag-positive cells for GFP-Rad9 foci allowed a comparison of transfected and untransfected cells within the same population. Untransfected cells exhibited an induction of GFP-Rad9 foci formation in response to aphidicolin or UV and this remained largely unaffected by expression of Flag-Rad17 (Fig. 2C,D). However, Flag-Rad17^{AA}-expressing cells displayed a reduced ability to form aphidicolin and UV-induced GFP-Rad9 foci compared with control cells expressing Flag-Rad17 (Fig. 2C,D). Expression of Flag-Rad17^{AA} resulted in an increased number of cells that exhibit Rad9 foci in the absence of damaging agents. Given that Rad17^{AA} expression induces genomic instability in the absence of exogenous stress (Wang et al., 2006), the increased number of Flag- Rad17^{AA} cells that display Rad9 foci in the absence of UV or aphidicolin probably reflects recruitment of Rad9 to sites of endogenous DNA damage induced by expression of Flag-Rad17^{AA}.

To discount the possibility that the reduced ability to form GFP-Rad9 foci in Flag-Rad17^{AA} cells is a consequence of expressing mutant Rad17 in the presence of endogenous Rad17, we expressed siRNA-resistant wild-type or mutant versions of Flag-Rad17 in cells that had been transfected with Rad17 siRNA. Staining with Flag antibodies identified cells that expressed siRNA-resistant Flag-Rad17 in the presence of Rad17 knockdown. Whereas expression of siRNA-resistant Flag-Rad17 restored DNA-damage-induced GFP-Rad9 foci formation in Rad17 downregulated cells, expression of siRNA-resistant Flag-Rad17^{AA} failed to restore the defect caused by downregulation of endogenous Rad17 (supplementary material Fig. S2). Together, these data argue that the observed phenotype of Flag-Rad17^{AA} expression is not due to the presence of endogenous Rad17 and illustrate that phosphorylation of Rad17 on Ser635 and/or Ser645 affects the ability of Rad9 to form foci in response to endogenous or exogenous genotoxic stress.

Disruption of ATR function results in a decreased number of cells that exhibit Rad9 foci in response to UV and replication stress

ATR and the 9-1-1 complex are recruited independently to sites of DNA damage (Kondo et al., 2001; Lisby et al., 2004; Melo et al., 2001; You et al., 2002; Zou et al., 2002). However, in vertebrates,

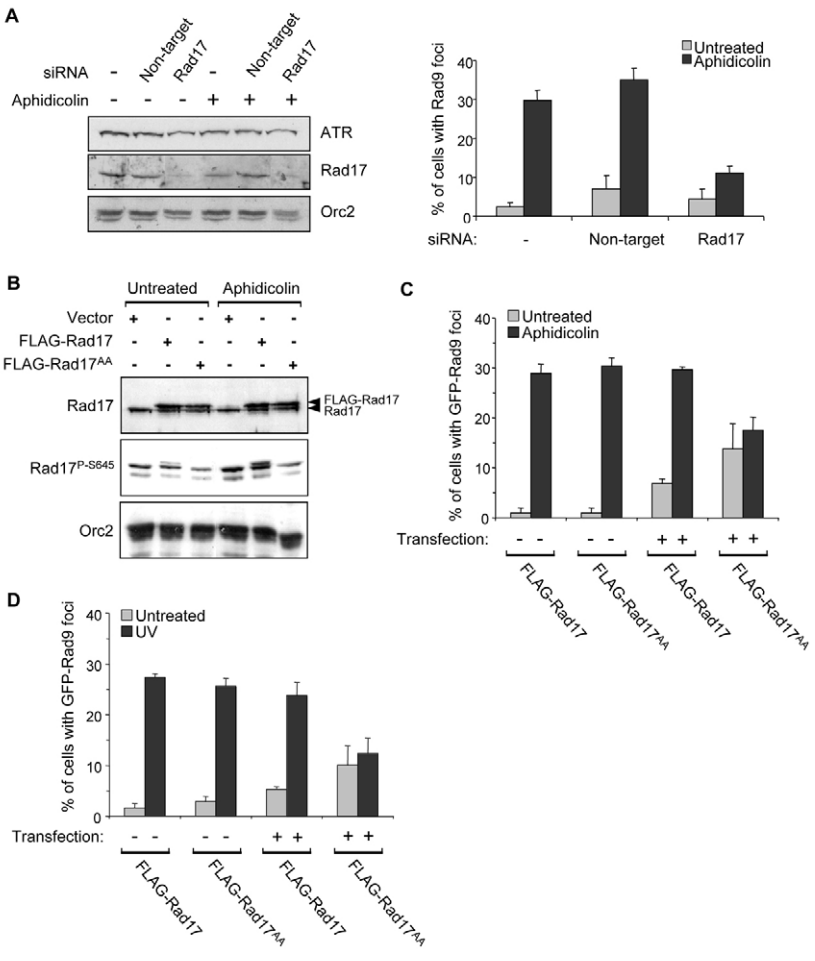

Fig. 2. Rad17 is required for Rad9 to form foci in response to DNA damage. (A) HeLa cells were transfected with siRNA oligonucleotides as indicated and were left untreated or exposed to aphidicolin. Whole cell extracts were prepared for western blotting (left panel) and the percentage of cells exhibiting more than ten Rad9 foci was determined (right panel). (B) U2OS cells expressing GFP-Rad9 were transfected with empty vector, or vector containing Flag-Rad17 or Flag-Rad17^{AA}. Cells were left untreated or exposed to aphidicolin. Chromatin fractions were prepared and extracts subjected to western blotting using antibodies as indicated. (C) U2OS cells stably expressing GFP-Rad9 were transfected with Flag-Rad17 or Flag-Rad17^{AA} constructs prior to treating cells with aphidicolin. Flag-positive (transfected) or Flag-negative (untransfected) cells were identified by immunofluorescence and cells scored for GFP-Rad9 foci. (D) U2OS cells stably expressing GFP-Rad9 were transfected as in C, after which cells were treated with UV. Flag-positive (transfected) or Flag-negative (untransfected) cells were identified by immunofluorescence and cells were scored for GFP-Rad9 foci.

much of the literature describing the relationship between these two DNA damage sensors has focused on examining enrichment of proteins in chromatin fractions isolated from cells following exposure to genotoxic stress (You et al., 2002; Zou et al., 2002). Consistent with these reports, we also observed that repression of ATR levels using siRNA did not affect enrichment of Rad9 in chromatin-containing fractions following exposure of cells to UV radiation (Fig. 3A).

Our observations that Flag-Rad17^{AA} expression results in a reduced number of cells that exhibit DNA damage or replication-stress-induced Rad9 foci led us to assess the requirement for ATR in Rad9 foci formation following genotoxic stress. As predicted, repression of Rad9 expression by siRNA abrogated formation of UV-induced Rad9 foci formation (Fig. 3B). Consistent with our biochemical data (Fig. 3A), UV-induced Rad9 foci formation was still apparent in cells that had been transfected with ATR siRNA. However, in these experiments we observe a modest but nonetheless significant decrease from 32% to 24% of cells that exhibited UV-induced Rad9 foci in the absence of ATR (Fig. 3B). Importantly, UV-induced RPA foci remained intact following transfection with ATR or Rad9 siRNA (Fig. 3C), arguing that the reduction of Rad9 foci is not a consequence of inefficient ssDNA formation and/or recruitment of RPA to sites of DNA damage. Although we observe a reproducible decrease in efficiency of Rad9 foci formation in ATR siRNA cells, this is not as dramatic as that achieved by overexpression of Flag-Rad17^{AA}. Therefore, we cannot formally rule out additional effects of Rad17 phosphorylation on Rad9 foci formation in response to UV radiation. Alternatively, these observations could be explained by increased genomic instability in cells lacking ATR (Paulsen and Cimprich, 2007).

Similarly to UV-induced DNA damage, repression of ATR using siRNA did not affect enrichment of Rad9 in chromatin-containing fractions following administration of aphidicolin (Fig. 3D). However, similarly to UV-induced damage, we also detected a decrease in the number of cells that exhibited aphidicolin-induced Rad9 or GFP-Rad9 foci formation in the absence of ATR (Fig. 4E and data not shown).

To establish whether the absence of an absolute requirement for ATR in loading Rad9 onto chromatin or formation of Rad9 foci following administration of aphidicolin could be explained by a functional redundancy between ATR, ATM and/or DNA-activated protein kinase (DNA-PK), we combined siRNA of ATR with specific inhibitors of ATM (Hickson et al., 2004) and DNA-PK (Veuger et al., 2003) prior to assessing either enrichment of Rad9 in chromatin-containing cellular fractions, or formation of Rad9 foci following administration of aphidicolin. Loading of Rad9 onto chromatin following administration of aphidicolin remained intact in cells subjected to ATR siRNA either in the absence or presence of ATM and DNA-PK inhibitors (Fig. 3D). Similarly, addition of ATM and/or DNA-PK inhibitors to cells that had been treated with ATR siRNA oligonucleotides did not result in a further dramatic decrease in the number of cells that exhibited Rad9 foci (Fig. 3E). Together, these data argue that functional redundancy is not the reason for the observation that Rad9 foci formation is not completely dependent on ATR.

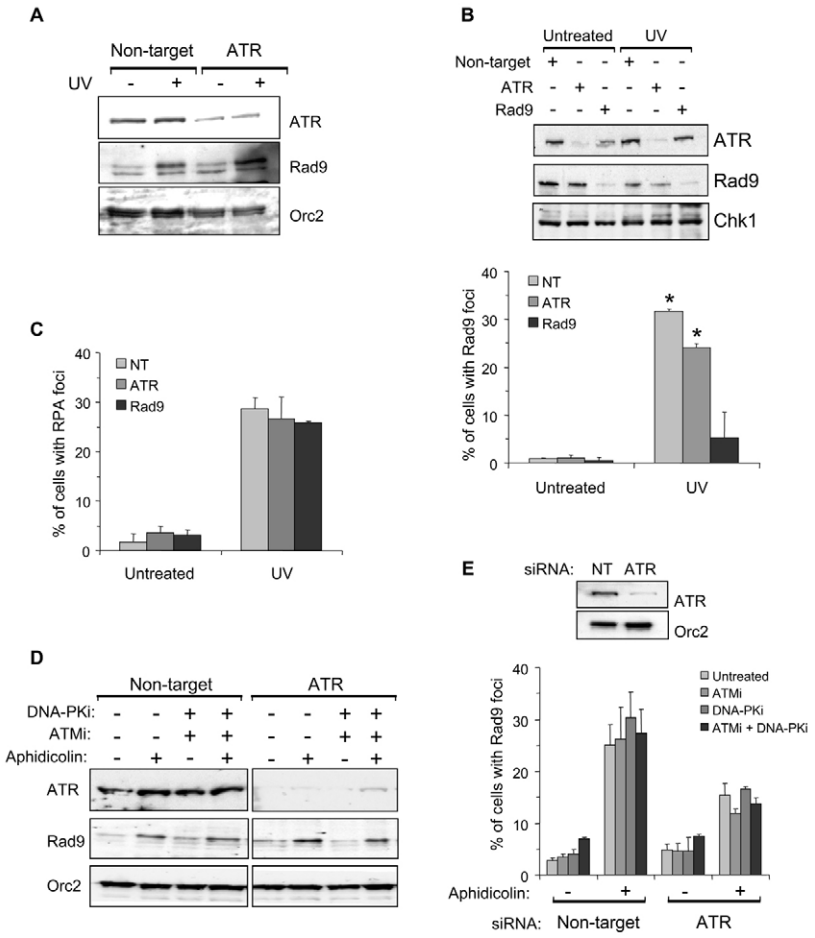

Fig. 3. ATR is required for formation of a subset of UV- and aphidicolin-induced Rad9 foci. (A) HeLa cells were transfected with siRNA oligonucleotides as indicated, exposed to UV and chromatin fractions prepared. Western blot analysis was performed using the indicated antibodies. (B) HeLa cells were transfected with siRNA oligonucleotides as indicated. Cells were treated with UV and harvested for western blotting (upper panel). The percentage of cells exhibiting more than ten Rad9 foci was determined by immunofluorescence (lower panel). *P=0.017 between these two data points indicating statistical significance at the 95% confidence level. (C) Cells were transfected with siRNA and treated as in B. The percentage of cells exhibiting more than ten RPA (p34 subunit) foci was determined by immunofluorescence. (D) HeLa cells were transfected with siRNA oligonucleotides as indicated and 72 hours after transfection were treated with a combination of ATM (10 μM) and DNA-PK (1 μM) inhibitors, or left untreated for 1 hour prior to exposure to aphidicolin. Cells were fractionated to obtain chromatin-enriched proteins and western blotting performed using the indicated antibodies. (E) HeLa cells were transfected with siRNA oligonucleotides as indicated and whole cell extracts prepared for western blotting (upper panel). In parallel, cells were treated with ATM (10 μM) and/or DNA-PK (1 μM) inhibitors, or left untreated prior to exposure to aphidicolin. The percentage of cells exhibiting more than ten Rad9 foci was determined.

ATR and Rad17 phosphorylation influence Rad9 retention at DNA damage sites

Our findings that the number of cells that display Rad9 foci is reduced by the absence of ATR prompted us to consider whether ATR might have an alternative effect on 9-1-1 function other than facilitating its ability to be recruited to sites of DNA damage. For example, if ATR is required to amplify or retain Rad9 at sites of DNA damage, it is conceivable that Rad9 might still transiently

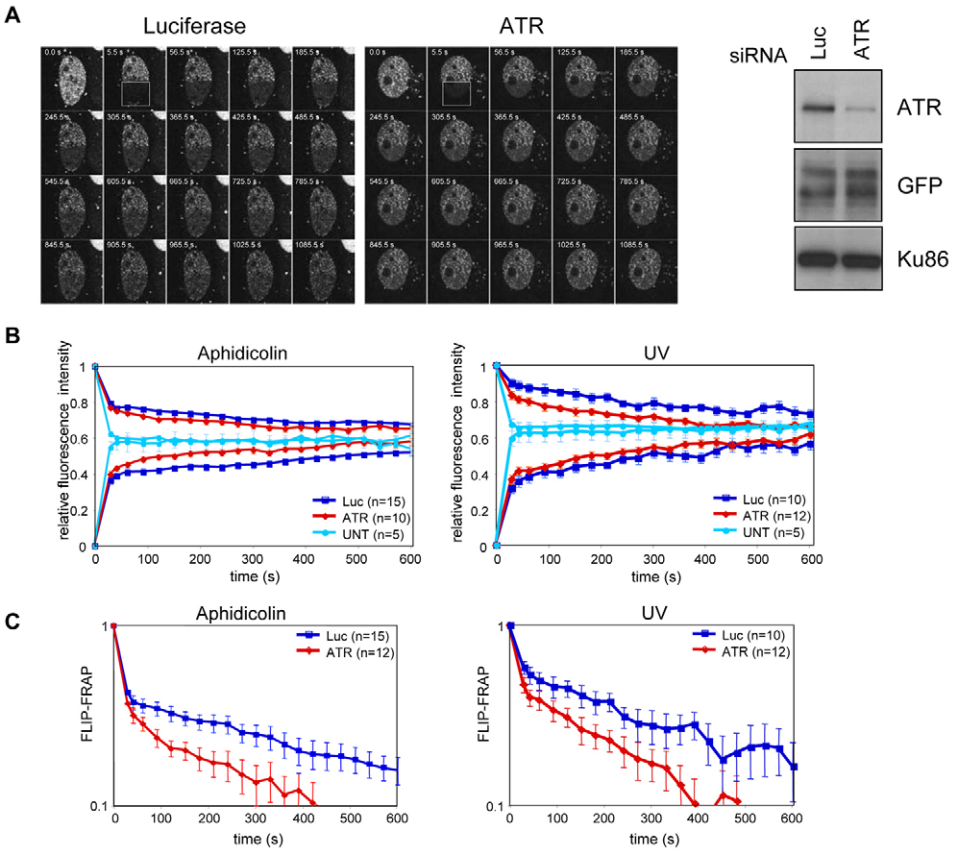

Fig. 4. ATR influences the retention time of GFP-Rad9 in damage-induced foci. (A) U2OS cells expressing GFP-Rad9 were transfected with ATR or Luciferase siRNA oligonucleotides, and treated with aphidicolin. Half the nucleus containing GFP-Rad9 foci (see rectangle) was bleached for 2.7 seconds at 100% laser intensity, after which redistribution of fluorescence was monitored by recording images every 60 seconds. Western blot analysis of cell extracts from a representative experiment is illustrated (right panel). (B) Quantification of simultaneous FLIP-FRAP experiment as in A, with the exception that the cells were imaged every 30 seconds. Cells were treated with aphidicolin (left panel) or UV (right panel), after which FLIP was measured in the unbleached part of the cell and FRAP was measured in the bleached part of the cell. Control cells (UNT) are either left untreated or treated with damaging agents but not displaying GFP-Rad9 foci. The mean of the data points of individual cells analysed is illustrated (*n*=number of cells) with error bars representing the s.e.m. (C) Difference in relative fluorescence in bleached and unbleached parts of the nucleus from B, plotted against time. Error bars represent twice the s.e.m.

interact with DNA lesions in the absence of this kinase. Therefore, we assessed whether Rad9 proteins within established foci are immobile or whether these foci are more dynamic structures in which Rad9 proteins turnover, a process that could possibly be affected by ATR. To assess this, we used simultaneous fluorescence loss in photobleaching (FLIP) and fluorescence recovery after photobleaching (FRAP) technology, an assay used in living cells that has been successfully used to monitor protein redistribution in real time (Essers et al., 2005; Hoogstraten et al., 2002; Lukas et al., 2003; Mattern et al., 2004; Pryde et al., 2005). In these experiments, U2OS cells expressing GFP-Rad9 were transfected with control or ATR siRNA oligonucleotides. Subsequently, cells were treated with either UV or aphidicolin, half the nucleus containing the resulting GFP-Rad9 foci was photobleached, and cells were followed in real time by videomicroscopy (Fig. 4A). The redistribution of fluorescence was monitored by measuring FRAP in the bleached part and FLIP in the unbleached part of the nucleus and the change in fluorescence versus time, indicative of GFP-Rad9 turnover, was quantified (Fig. 4B).

Whereas GFP-Rad9 was highly mobile in undamaged cells and cells without foci, turnover of GFP-Rad9 within DNA-damage-induced foci was comparatively slow. In addition, the FLIP and FRAP curves of control-transfected cells did not converge during the time span of our experiments (800-1000 seconds), suggesting the presence of a stably associated Rad9 fraction in damaged areas (Fig. 4B and data not shown). Similarly to luciferase-transfected control cells, UV- and aphidicolin-induced foci formation also resulted in a decrease in the mobility of GFP-Rad9 in cells transfected with ATR siRNA oligonucleotides. However, in this case, the FLIP-FRAP curves almost fully converged, suggesting the absence of a long-lived immobile fraction of GFP-Rad9 in foci when ATR protein levels are repressed (Fig. 4B). The time-lapse images in Fig. 4A additionally demonstrate faster redistribution of fluorescence within damage-induced foci upon repression of ATR protein levels compared with control cells, which is confirmed by the slopes of the FLIP-FRAP curves (Fig. 4B).

In addition, the difference in relative fluorescence intensities between the FRAP and FLIP areas was plotted against time, and the time it took to reach full redistribution (>90%) was determined as a measure of mobility. Full redistribution of GFP-Rad9 within DNA-damage-induced foci was not reached during the time course of our experiments (800-1000 seconds) (Fig. 4C and data not shown). However, following repression of ATR levels using siRNA, full redistribution was reached within 450-500 seconds after bleaching, indicating an increase in protein mobility upon downregulation of ATR (Fig. 4C). Together, these results demonstrate that Rad9 proteins display a higher turnover in cells where GFP-Rad9 foci formation induced by DNA damage is not affected by the absence of ATR.

Our results suggest that the effect of ATR on the stability of GFP-Rad9 in damage-induced foci is mediated by phosphorylation of Rad17. To test whether this is indeed the case, we performed simultaneous FLIP-FRAP measurements on UV-induced GFP-Rad9 foci in cells expressing Flag-Rad17 or Flag-Rad17^{AA}. Although wild-type Flag-Rad17 did not interfere with the slow dynamic behaviour of GFP-Rad9 within foci, expression of Flag-Rad17^{AA} resulted in a similar phenotype to that observed upon downregulation of ATR: an increased mobility of GFP-Rad9 within foci (Fig. 5A). Furthermore, full redistribution of GFP-Rad9 in UV-induced foci was reached within 450-500 seconds after the bleach pulse upon Flag-Rad17^{AA} expression, whereas

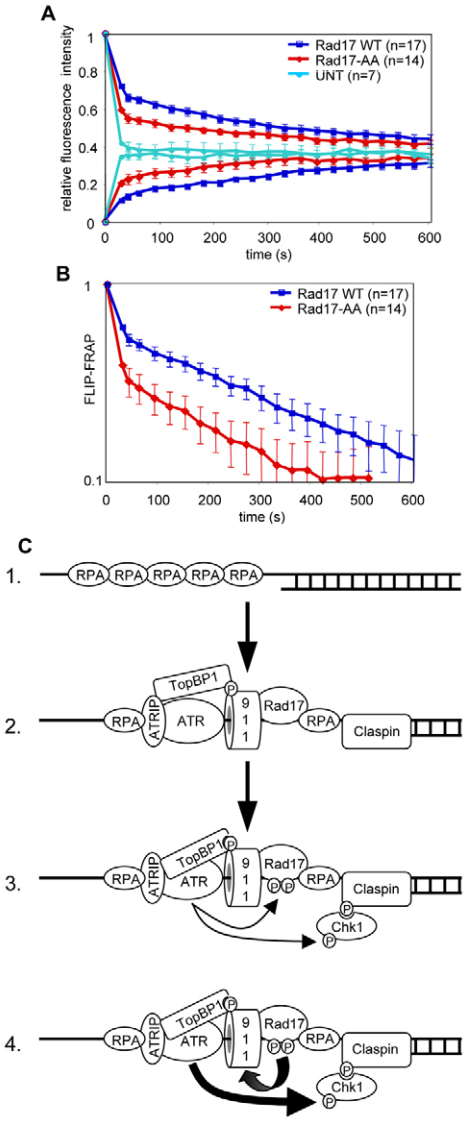

Fig. 5. Rad17 phosphorylation at Ser635 and Ser645 decreases the mobility of GFP-Rad9 in damage-induced foci. U2OS cells expressing GFP-Rad9 were transfected with Flag-Rad17 or Flag-Rad17^{AA} constructs, together with mCherry-C1, to detect transfected cells. Cells were left untreated (UNT) or treated with UV and FLIP-FRAP analysis was performed on red cells. (A) Quantification of FLIP and FRAP as described in Fig. 4B. (B) Difference in relative fluorescence, plotted against time, as described in Fig. 4C. (C) ATR and Rad17 collaborate in modulating Rad9 localisation at sites of DNA damage. ssDNA generated as a result of DNA damage or replication stress is recognised by RPA (1). Recognition of ssDNA by RPA leads to the independent recruitment of ATR and Rad17 to DNA lesions. Rad17 loads the 9-1-1 complex at sites of ssDNA and facilitates activation of ATR through an interaction with TopBP1 (2). ATR subsequently phosphorylates Claspin, which acts to recruit Chk1 and promote its phosphorylation by ATR. ATR also phosphorylates Rad17 (3). ATR-mediated phosphorylation of Rad17 stabilises the 9-1-1 complex at sites of DNA lesions. This could in turn result in the maintenance of activated ATR and continued checkpoint signalling until DNA damage is repaired (4).

this equilibrium was not reached in control cells (Fig. 5B). Taken together, these data demonstrate that Rad17 affects the turnover of Rad9 molecules in foci, a process that critically depends on ATR-mediated phosphorylation.

Discussion

In this report we present data that suggest a model in which Rad17 and ATR collaborate in regulating the localisation of the 9-1-1 complex at sites of damage. The ability of Rad9 to form DNA-damage-induced nuclear foci in the absence of ATR has not previously been reported in mammalian cells. However, analysis of *Saccharomyces cerevisiae* 9-1-1 (Ddc1-Rad17-Mec3) has revealed that formation of DNA DSB-induced Ddc1-Rad17-Mec3 nuclear foci can still occur in the absence of functional ATR (Mec1p) (Lisby et al., 2004; Melo et al., 2001). In accordance with these findings, we also observe Rad9 foci formation in cells that have been treated with ATR siRNA following UV-induced DNA damage or replication stress (Figs 3 and 4). Taken together with our biochemical data that illustrate ATR is not required for Rad9 enrichment on chromatin in response to DNA damage or replication stress (Fig. 3A,D), our results support the currently accepted dogma that ATR is not required for 9-1-1 to access sites of DNA damage. Importantly, however, our experiments studying the dynamic behaviour of GFP-Rad9 foci by live-cell imaging suggest that although ATR does not influence the initial recruitment of Rad9 to DNA lesions, it does have an impact on the ability of this protein complex to be maintained within nuclear foci.

As the number of reports examining DNA-damage checkpoint regulation in living cells is limited (Bekker-Jensen et al., 2005; Lukas et al., 2003; Lukas et al., 2004a), our experiments provide valuable insight into understanding this complex process, which appears to be more dynamic than originally anticipated (Lukas et al., 2004b). Although the Chk2 and Chk1 effector kinase are phosphorylated at sites of damage, induction of genotoxic stress does not lead to their immobilisation, demonstrating the dynamic nature of these proteins (Lukas et al., 2003; Smits et al., 2006) (V.A.J.S. and D.O.W., unpublished). By contrast, several checkpoint proteins involved in the early stages of the checkpoint response, such as NBS1, MDC1 and 53BP1, are transiently immobilised in DNA damaged areas (Bekker-Jensen et al., 2005; Lukas et al., 2003; Lukas et al., 2004a). The observed immobilisation of GFP-Rad9 in DNA-damage-induced foci is in agreement with the suggested function of Rad9 as a DNA-damage sensor protein, which contributes to activation of the checkpoint upon recruitment to sites of damage. However, the observed function of ATR in Rad9 turnover in established foci was unexpected in light of previous reports (Kondo et al., 2001; Lisby et al., 2004; Melo et al., 2001; You et al., 2002; Zou et al., 2002), and demonstrates a more subtle control of checkpoint regulation than was initially envisaged.

These findings are of particular interest given the emerging theme that signalling DNA damage is not a purely linear pathway and that a variety of parallel mechanisms exist that contribute towards maintenance or amplification of the signal. For example, although histone H2AX phosphorylation is not essential for the initial recruitment of certain DNA-damage signalling proteins to DNA DSBs, it is required for these proteins to persist at break sites and form DNA-damage-induced nuclear foci (Celeste et al., 2003). Similarly, ATM-mediated phosphorylation of H2AX in response to DNA DSBs has been proposed to amplify the initial signal generated at a break site by recruiting additional ATM via an interaction with the Mre11-Rad50-Nbs1-Mdc1 protein complex (Stucki et al., 2005). Therefore, one possible interpretation of our data is that activation of ATR serves as a signal to 9-1-1 that subsequently stabilises the interaction of this protein complex with sites of DNA damage, resulting in amplification or maintenance of the checkpoint signal.

A link between ATR and the ability of 9-1-1 to be maintained at sites of genotoxic stress is further supported by our observations that expression of Rad17 that is unable to be phosphorylated by ATR results in a similar increased dynamic behaviour of Rad9 within foci. How DNA-damage-induced phosphorylation of Rad17 contributes towards the regulation of 9-1-1 is a matter of debate. The observation that ATR is not required for enrichment of 9-1-1 on chromatin in response to genotoxic stress argues against phosphorylation of Rad17 contributing towards regulating the access of 9-1-1 to sites of DNA damage (You et al., 2002; Zou et al., 2002). Conversely, phosphorylation of Rad17 on Ser635 and Ser645 promotes an interaction with the 9-1-1 complex, raising the possibility that ATR-mediated phosphorylation of Rad17 can influence the ability of 9-1-1 to interact with sites of DNA damage (Bao et al., 2001). Together our results unify these findings and demonstrate that although phosphorylation of Rad17 by ATR is not required for 9-1-1 to access DNA damage sites per se, it does contribute to retention of 9-1-1 within the vicinity of the DNA lesion.

The 9-1-1 complex facilitates activation of ATR not through promoting its interaction with DNA damage sites, but by recruiting the ATR activating protein TopBP1 to sites of DNA damage (Delacroix et al., 2007; Kumagai et al., 2006; Lee et al., 2007). It is interesting to speculate, therefore, that the initial activation of ATR by TopBP1 results in phosphorylation of Rad17 and subsequent stabilisation of the Rad17–9-1-1–TopBP1 complex at DNA lesions. This in turn could result in the maintenance of activated ATR and continued checkpoint signalling until DNA damage is repaired (Fig. 5C). This hypothesis is particularly interesting in light of recent observations illustrating that ATR-mediated phosphorylation of Rad17 is not absolutely required for activation of Chk1 in response to replication fork stalling, but is instead required for the maintenance of the checkpoint following removal of stress (Wang et al., 2006). Taken together, our findings might be indicative of a biphasic response to genotoxic stress that constitutes an initial recruitment of signalling proteins to DNA damage followed by subsequent regulation of checkpoint proteins at damage sites to maintain the checkpoint.

Materials and Methods

Cell culture and maintenance

HeLa and Swiss 3T3 cells obtained from the European Collection of Cell Cultures (Health Protection Agency, Porton Down, Wiltshire, UK) and U2OS cells were grown using standard procedures. U2OS cells stably expressing eGFP-HA_2-Rad9 were grown in standard medium supplemented with 700 μg/ml geneticin (G418). The ATM inhibitor KU-55933 (Hickson et al., 2004) and DNA-PK inhibitor KU00557788 (Veuger et al., 2003) were pre-incubated with cells for 1 hour before UV treatment, and used at concentrations of 10 μM and 1 μM, respectively. UV was administered using a StrataLinker 2400 source (Stratagene) or a 254 nm UV-C lamp (Philips) at 20 J/m^2 and cells were processed 1 hour post treatment. To stall replication forks, asynchronously growing cells were incubated in 5 μg/ml of aphidicolin (Sigma) for 20 hours prior to processing of samples.

Antibodies

Antibodies obtained from commercial sources were as follows: Chk1 (Cell Signalling Technology), Chk1 pS317 (Bethyl), Flag (M2; Sigma), Orc2 (BD Pharmingen), Rad9 (Novus Biologicals), Rad17 pS645 (Cell Signalling Technology), RPA (Neomarkers) and RPA (Oncogene). The following antibodies were obtained from Santa Cruz Biotechnology: ATR (N-19), Chk1 (G-4), Ku86 (C-20), Rad1 (N-18), Rad9 (C-20), Rad9 (M-389) and Rad17 (H-300). Rabbit polyclonal anti-Hus1, anti-Rad9 and anti-GFP antibodies were a gift from Raimundo Freire (Unidad de Investigación HUC, Tenerife, Spain).

Plasmids and site-directed mutagenesis

pmCherry-C1 was kindly provided by Roger Tsien (Department of Pharmacology and Howard Hughes Medical Institute, University of California, San Diego, CA). pPCMV eGFP-spectrin has been previously described (Kalejta et al., 1997). hRad9 cDNA was digested from pGEX-4T3-GST-Rad9, kindly provided by Raimundo Freire, and cloned into the multiple cloning site of pcDNA3.1$^+$ (Invitrogen). eGFP-HA was amplified by PCR from pEGFP-C2 (Clontech) and inserted in frame into pcDNA3.1$^+$Rad9 to generate pcDNA3.1$^+$eGFP-HA-Rad9.

A full-length Rad17 clone was purchased from Open Biosystems (Clone ID: 5170876, code: MHS1010-7508047). Rad17 was subcloned into the *Eco*R1 and *Kpn*1 sites of the pCMV-Flag-2 plasmid (Sigma). The full-length cDNA and linker regions were confirmed to be correct by sequencing. The pCMV-Flag-Rad17 construct was subjected to PCR amplification with the following primers to incorporate the S635A mutation: 5′-TCTCTTCCTTTGGCTCAGAATAGTGCC-3′ and 5′-GGCACTATTC-TGAGCCAAAGGAAGAGA-3′. PCR products were digested with the methylation-sensitive restriction enzyme *Dpn*1 to eliminate any original plasmid. To create the second mutation (S645A) we followed the same process using the following primers: 5′-GAACTGCCTGCTGCCCCAGCCCCAGC-3′ and 5′-GCTGGGGCTGGGC-AGCAGGCAGTTC-3′.

Flag-Rad17 and Flag-Rad17^{AA} constructs that are resistant to siRNA were produced using the same methodology to introduce conservative mutations in the third nucleotide of each codon contained within the Rad17 siRNA target sequence. Primers used in site-directed mutagenesis were as follows: 5′-CCAGAAACCCAA-CACGAGCTAGCAGTGCATAAAAAGAAAATTG-3′ and 5′-TATGCACTGCTA-GCTCGTGTTGGGTTTCTGGTTTATATTTATCC-3′. Resulting Rad17 open reading frames, including the linker regions, were fully sequenced to confirm mutation of the relevant sites.

Transfection

siRNA oligonucleotides (Dharmacon Research) were transfected into cells using Oligofectamine (Invitrogen) according to the manufacturer's instructions, and as previously described (Adams et al., 2006; Dart et al., 2004; Smits et al., 2006). Cells were incubated for 72 hours after transfection prior to further analysis. Sequences of oligonucleotides were as follows: NT, UGCGACUAAACACAUCAAUUdTdT; Luc, CGUACGCGGAAUACUUCGAdTdT; ATR, CCUCCGUGAUGUUGCUUGA-dTdT; Rad9, GUCUUUCCUGUCUGUCUUCdTdT; Rad17, CAGACUGGGUU-GACCCAUCdTdT. Plasmid DNA was transfected into cells using lipofectamine (Fig. 2B) or the calcium phosphate transfection method (all other experiments). For stable expression of eGFP-HA-Rad9 in U2OS cells, positive clones were selected after a selection with G418 (1400 μg/ml) for 2 weeks.

For downregulating endogenous Rad17 while expressing siRNA-resistant Flag-Rad17 constructs, we transfected plasmid DNA into cells using FuGENE HD transfection reagent (Roche) according to the manufacturer's instructions. The next day, siRNA oligonucleotides were transfected as described above and cells were harvested 72 hours after transfection.

Immunofluorescence

Cells were grown as monolayers on glass coverslips. For detection of endogenous Rad9, cells were pre-extracted in Buffer 1 (1% Triton X-100, 10 mM HEPES pH 7.4, 10 mM NaCl, 3 mM $MgCl_2$) for 5 minutes at 4°C. Cells were then fixed in 4% paraformaldehyde for 10 minutes at 4°C and finally permeabilised further in Buffer 2 (0.5% Triton X-100, 20 mM HEPES pH 7.4, 50 mM NaCl, 3 mM $MgCl_2$, 300 mM sucrose) for 5 minutes at 4°C. Cells containing more than ten foci were scored as Rad9 positive. This number reflects the DNA-damage-inducible population within experiments. In all instances, error bars on graphs represent the s.e.m. of three independent experiments. For detection of RPA, cells were fixed in 4% paraformaldehyde for 10 minutes at 4°C followed by permeabilisation in 0.5% Triton X-100 for 5 minutes at 4°C. Immunofluorescence was detected using an Axioscope 2 fluorescent microscope equipped with Axiovision imaging software (Zeiss). For detection of GFP-Rad9 in U2OS cells, living cells were studied, or cells were fixed in 2% paraformaldehyde containing 0.2% Triton X-100 for 20 minutes at room temperature and then permeabilised with 0.1% Triton X-100 for 5 minutes at room temperature.

Imaging and FLIP-FRAP of GFP-Rad9 were performed on a Confocal Laser Scanning Microscope LSM 510 (Zeiss), equipped with a 488 nm Ar laser and a 505-550 nm band pass filter. In Fig. 5, cells were co-transfected with mCherry-C1, kindly provided by Roger Tsien. Red fluorescence was selected using a 514 nm Ar laser and 575-615 nm band pass filter, after which the FLIP-FRAP measurements of GFP-Rad9 were performed, as described, in mCherry-positive cells.

Cell fractionation and western blotting

Whole-cell extracts were prepared by washing cultures in PBS before boiling cells in Laemmli buffer for 10 minutes. Protein concentrations were determined using the Lowry protein assay. Biochemical fractionation of cells was performed as previously described (Dart et al., 2004; Mendez and Stillman, 2000).

Cell cycle analysis

For cell cycle analysis, cells were collected by trypsinisation and fixed in 70% ethanol at 4°C for a minimum of 2 hours. After fixation, cells were washed with PBS and the DNA was stained with propidium iodide. Cell cycle profiles were analysed by flow cytometry using an Epics XL-MCL from Beckman Coulter.

Photobleaching experiments

In the simultaneous FLIP-FRAP experiments, half of the nucleus was bleached for 2.7 seconds at 100% laser intensity, which irreversibly bleaches all GFP-Rad9 molecules. Subsequently, the redistribution of fluorescence in the nucleoplasm and the exchange of bleached and unbleached molecules between foci and nucleoplasm was monitored by taking confocal images at fixed time intervals (60 seconds for Fig. 4A and 30 seconds for Fig. 4B,C, and Fig. 5A,B). The relative intensities I_R of the bleached and unbleached halves of the cell were calculated as $I_R=(I_t–I_0)/(I_{t<0}–I_0)$, where I_t is the intensity measured at consecutive time points, I_0 is the intensity of the bleached part of the nucleus immediately after bleaching and $I_{t<0}$ is the intensity before bleaching (Fig. 4B and Fig. 5A). The fluorescence before bleaching ($I_{t<0}$) was set to 1 and the intensity immediately after bleaching (I_0) was set to 0. The difference in relative fluorescence in bleached and unbleached parts of the nucleus was plotted against time (Fig. 4C and Fig. 5B).

We thank Graeme Smith (KuDOS Pharmaceuticals, Cambridge, UK) for ATM and DNA-PK inhibitors. We also thank Roger Tsien and Raimundo Freire for reagents, and members of the Genetics Department of Erasmus MC for helpful discussions. V.A.J.S. thanks Steve Jackson and Julia Coates for support during early stages of this work. We also thank Liliana Malinovska for helping generate the siRNA-resistant Flag-Rad17 constructs. This work was supported by the integrated project 512113 from the European Commission (R.K.), the Netherlands Genomics Initiative/Netherlands Organization for Scientific Research (N.W.O., R.K.), Cancer Research UK project grant C1521/A5207 (A.L.M.), University of Oxford Clarendon Scholarship (I.A.), the Association for International Cancer Research 05-005 (V.A.J.S.) and the Dutch Cancer Society EMCR 2005-3412 (V.A.J.S.).

References

Abraham, R. T. (2001). Cell cycle checkpoint signaling through the ATM and ATR kinases. *Genes Dev.* **15**, 2177-2196.

Adams, K. E., Medhurst, A. L., Dart, D. A. and Lakin, N. D. (2006). Recruitment of ATR to sites of ionising radiation-induced DNA damage requires ATM and components of the MRN protein complex. *Oncogene* **25**, 3894-3904.

Ball, H. L., Myers, J. S. and Cortez, D. (2005). ATRIP binding to replication protein A-single-stranded DNA promotes ATR-ATRIP localization but is dispensable for Chk1 phosphorylation. *Mol. Biol. Cell* **16**, 2372-2381.

Bao, S., Tibbetts, R. S., Brumbaugh, K. M., Fang, Y., Richardson, D. A., Ali, A., Chen, S. M., Abraham, R. T. and Wang, X. F. (2001). ATR/ATM-mediated phosphorylation of human Rad17 is required for genotoxic stress responses. *Nature* **411**, 969-974.

Bekker-Jensen, S., Lukas, C., Melander, F., Bartek, J. and Lukas, J. (2005). Dynamic assembly and sustained retention of 53BP1 at the sites of DNA damage are controlled by Mdc1/NFBD1. *J. Cell Biol.* **170**, 201-211.

Bermudez, V. P., Lindsey-Boltz, L. A., Cesare, A. J., Maniwa, Y., Griffith, J. D., Hurwitz, J. and Sancar, A. (2003). Loading of the human 9-1-1 checkpoint complex onto DNA by the checkpoint clamp loader hRad17-replication factor C complex *in vitro*. *Proc. Natl. Acad. Sci. USA* **100**, 1633-1638.

Byun, T. S., Pacek, M., Yee, M. C., Walter, J. C. and Cimprich, K. A. (2005). Functional uncoupling of MCM helicase and DNA polymerase activities activates the ATR-dependent checkpoint. *Genes Dev.* **19**, 1040-1052.

Celeste, A., Fernandez-Capetillo, O., Kruhlak, M. J., Pilch, D. R., Staudt, D. W., Lee, A., Bonner, R. F., Bonner, W. M. and Nussenzweig, A. (2003). Histone H2AX phosphorylation is dispensable for the initial recognition of DNA breaks. *Nat. Cell Biol.* **5**, 675-679.

Chen, Y. and Sanchez, Y. (2004). Chk1 in the DNA damage response: conserved roles from yeasts to mammals. *DNA Repair (Amst.)* **3**, 1025-1032.

Dart, D. A., Adams, K. E., Akerman, I. and Lakin, N. D. (2004). Recruitment of the cell cycle checkpoint kinase ATR to chromatin during S-phase. *J. Biol. Chem.* **279**, 16433-16440.

Delacroix, S., Wagner, J. M., Kobayashi, M., Yamamoto, K. and Karnitz, L. M. (2007). The Rad9-Hus1-Rad1 (9-1-1) clamp activates checkpoint signaling via TopBP1. *Genes Dev.* **21**, 1472-1477.

Ellison, V. and Stillman, B. (2003). Biochemical characterization of dna damage checkpoint complexes: clamp loader and clamp complexes with specificity for 5′ recessed DNA. *PLoS Biol.* **1**, E33.

Essers, J., Theil, A. F., Baldeyron, C., van Cappellen, W. A., Houtsmuller, A. B., Kanaar, R. and Vermeulen, W. (2005). Nuclear dynamics of PCNA in DNA replication and repair. *Mol. Cell. Biol.* **25**, 9350-9359.

Hickson, I., Zhao, Y., Richardson, C. J., Green, S. J., Martin, N. M., Orr, A. I., Reaper, P. M., Jackson, S. P., Curtin, N. J. and Smith, G. C. (2004). Identification and characterization of a novel and specific inhibitor of the ataxia-telangiectasia mutated kinase ATM. *Cancer Res.* **64**, 9152-9159.

Hoogstraten, D., Nigg, A. L., Heath, H., Mullenders, L. H., van Driel, R., Hoeijmakers, J. H., Vermeulen, W. and Houtsmuller, A. B. (2002). Rapid switching of TFIIH between RNA polymerase I and II transcription and DNA repair *in vivo*. *Mol. Cell* **10**, 1163-1174.

Jazayeri, A., Falck, J., Lukas, C., Bartek, J., Smith, G. C., Lukas, J. and Jackson, S. P. (2006). ATM- and cell cycle-dependent regulation of ATR in response to DNA double-strand breaks. *Nat. Cell Biol.* **8**, 37-45.

Kalejta, R. F., Shenk, T. and Beavis, A. J. (1997). Use of a membrane-localized green fluorescent protein allows simultaneous identification of transfected cells and cell cycle analysis by flow cytometry. *Cytometry* **29**, 286-291.

Kastan, M. B. and Bartek, J. (2004). Cell-cycle checkpoints and cancer. *Nature* **432**, 316-323.

Kondo, T., Wakayama, T., Naiki, T., Matsumoto, K. and Sugimoto, K. (2001). Recruitment of Mec1 and Ddc1 checkpoint proteins to double-strand breaks through distinct mechanisms. *Science* **294**, 867-870.

Kumagai, A. and Dunphy, W. G. (2003). Repeated phosphopeptide motifs in Claspin mediate the regulated binding of Chk1. *Nat. Cell Biol.* **5**, 161-165.

Kumagai, A., Lee, J., Yoo, H. Y. and Dunphy, W. G. (2006). TopBP1 activates the ATR-ATRIP complex. *Cell* **124**, 943-955.

Lee, J., Kumagai, A. and Dunphy, W. G. (2007). The Rad9-Hus1-Rad1 checkpoint clamp regulates interaction of TopBP1 with ATR. *J. Biol. Chem.* **282**, 28036-28044.

Lisby, M., Barlow, J. H., Burgess, R. C. and Rothstein, R. (2004). Choreography of the DNA damage response; spatiotemporal relationships among checkpoint and repair proteins. *Cell* **118**, 699-713.

Lukas, C., Falck, J., Bartkova, J., Bartek, J. and Lukas, J. (2003). Distinct spatiotemporal dynamics of mammalian checkpoint regulators induced by DNA damage. *Nat. Cell Biol.* **5**, 255-260.

Lukas, C., Melander, F., Stucki, M., Falck, J., Bekker-Jensen, S., Goldberg, M., Lerenthal, Y., Jackson, S. P., Bartek, J. and Lukas, J. (2004a). Mdc1 couples DNA double-strand break recognition by Nbs1 with its H2AX-dependent chromatin retention. *EMBO J.* **23**, 2674-2683.

Lukas, J., Lukas, C. and Bartek, J. (2004b). Mammalian cell cycle checkpoints: signalling pathways and their organization in space and time. *DNA Repair (Amst.)* **3**, 997-1007.

Mattern, K. A., Swiggers, S. J., Nigg, A. L., Lowenberg, B., Houtsmuller, A. B. and Zijlmans, J. M. (2004). Dynamics of protein binding to telomeres in living cells: implications for telomere structure and function. *Mol. Cell. Biol.* **24**, 5587-5594.

Melo, J. and Toczyski, D. (2002). A unified view of the DNA-damage checkpoint. *Curr. Opin. Cell Biol.* **14**, 237-245.

Melo, J. A., Cohen, J. and Toczyski, D. P. (2001). Two checkpoint complexes are independently recruited to sites of DNA damage *in vivo*. *Genes Dev.* **15**, 2809-2821.

Mendez, J. and Stillman, B. (2000). Chromatin association of human origin recognition complex, cdc6, and minichromosome maintenance proteins during the cell cycle: assembly of prereplication complexes in late mitosis. *Mol. Cell. Biol.* **20**, 8602-8612.

O'Driscoll, M., Ruiz-Perez, V. L., Woods, C. G., Jeggo, P. A. and Goodship, J. A. (2003). A splicing mutation affecting expression of ataxia-telangiectasia and Rad3-related protein (ATR) results in Seckel syndrome. *Nat. Genet.* **33**, 497-501.

Paulsen, R. D. and Cimprich, K. A. (2007). The ATR pathway: fine-tuning the fork. *DNA Repair (Amst.)* **6**, 953-966.

Pryde, F., Khalili, S., Robertson, K., Selfridge, J., Ritchie, A. M., Melton, D. W., Jullien, D. and Adachi, Y. (2005). 53BP1 exchanges slowly at the sites of DNA damage and appears to require RNA for its association with chromatin. *J. Cell Sci.* **118**, 2043-2055.

Smits, V. A., Reaper, P. M. and Jackson, S. P. (2006). Rapid PIKK-dependent release of Chk1 from chromatin promotes the DNA-damage checkpoint response. *Curr. Biol.* **16**, 150-159.

Stucki, M., Clapperton, J. A., Mohammad, D., Yaffe, M. B., Smerdon, S. J. and Jackson, S. P. (2005). MDC1 directly binds phosphorylated histone H2AX to regulate cellular responses to DNA double-strand breaks. *Cell* **123**, 1213-1226.

Veuger, S. J., Curtin, N. J., Richardson, C. J., Smith, G. C. and Durkacz, B. W. (2003). Radiosensitization and DNA repair inhibition by the combined use of novel inhibitors of DNA-dependent protein kinase and poly(ADP-ribose) polymerase-1. *Cancer Res.* **63**, 6008-6015.

Wang, X., Zou, L., Lu, T., Bao, S., Hurov, K. E., Hittelman, W. N., Elledge, S. J. and Li, L. (2006). Rad17 phosphorylation is required for claspin recruitment and Chk1 activation in response to replication stress. *Mol. Cell* **23**, 331-341.

You, Z., Kong, L. and Newport, J. (2002). The role of single-stranded DNA and polymerase alpha in establishing the ATR, Hus1 DNA replication checkpoint. *J. Biol. Chem.* **277**, 27088-27093.

Zou, L. and Elledge, S. J. (2003). Sensing DNA damage through ATRIP recognition of RPA-ssDNA complexes. *Science* **300**, 1542-1548.

Zou, L., Cortez, D. and Elledge, S. J. (2002). Regulation of ATR substrate selection by Rad17-dependent loading of Rad9 complexes onto chromatin. *Genes Dev.* **16**, 198-208.

Zou, L., Liu, D. and Elledge, S. J. (2003). Replication protein A-mediated recruitment and activation of Rad17 complexes. *Proc. Natl. Acad. Sci. USA* **100**, 13827-13832.